

# A miniaturized non-dispersive infrared CO<sub>2</sub> sensor based on a 2D integrating cylinder

Xiaoning Jia<sup>1,2\*</sup>, Gunther Roelkens<sup>1,2</sup>, Roel Baets<sup>1,2</sup>, Joris Roels<sup>3</sup>

<sup>1</sup> Photonics Research Group, INTEC, Ghent University-imec, Technologiepark 126, 9052 Belgium

<sup>2</sup> Center for Nano- and Biophotonics, Ghent University, Belgium

<sup>3</sup> Melexis Technologies NV, Transportstraat 1, 3980 Tessenderlo, Belgium

xiaoning.jia@ugent.be

**Abstract:** We propose a novel, miniaturized NDIR CO<sub>2</sub> sensor based on a 2D integrating cylinder, realized using deep RIE and wafer bonding on silicon. The sensor has a detection limit down to  $\sim 250$ ppm, with a small footprint of only  $\sim 5\text{mm} \times 5\text{mm}$ . © 2019 The Author(s)

**OCIS codes:** 130.6010, 230.3120, 280.4788

## 1. Introduction

CO<sub>2</sub> sensors are widely applied, such as for air quality monitoring, greenhouse farming and industrial process control. Existing CO<sub>2</sub> sensors are either electrochemical or non-dispersive infrared (NDIR) sensors. Electrochemical sensors suffer from short-term stability, low durability and cross-response to other gases (eg. water vapour). In contrast, NDIR sensors offer long-term stability, high accuracy and high gas specificity [1]. However, NDIR sensors tend to be bulky as a long (several cm) interaction length is required to achieve ppm level detection [2]. Several efforts have been made to miniaturize NDIR sensors [3–5]. In this work we demonstrate a NDIR CO<sub>2</sub> sensor based on a 2D integrating cylinder implemented on a silicon substrate with  $\sim 250$ ppm detection limit. The use of an integrating cylinder allows for a miniaturized sensor with a long interaction length.

## 2. Sensor fabrication and experimental setup

Figure 1(a) shows the schematic of the integrating cylinder. The structure consists of two gold coated and bonded Si substrates. The bottom substrate consists of a cylindrical cavity with one input waveguide and two output waveguides (all  $300\ \mu\text{m}$  wide) defined by  $300\ \mu\text{m}$  Deep Reactive Ion Etching (DRIE), as shown in Fig 1(b). A thin layer of gold ( $\sim 300\text{nm}$ ) was then sputtered on the bottom substrate as well as on the (planar) top substrate. After gold deposition, the two substrates undergo Ar plasma treatment and are bonded using gold-to-gold direct bonding (at  $300^\circ\text{C}$ ,  $1\text{MPa}$  for 30 minutes). The fabricated sensor is shown in Fig. 1(c).

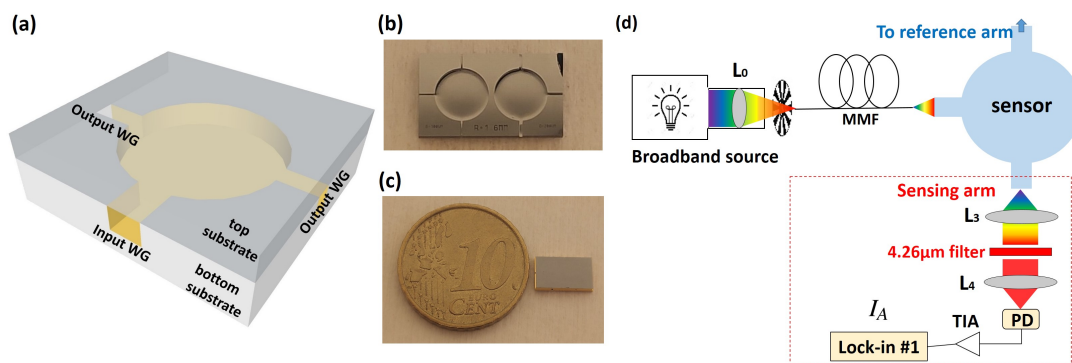


Fig. 1: (a) Sensor schematic. (b) DRIE etched cylindrical cavity with one input waveguide and two output waveguides (etch depth =  $300\ \mu\text{m}$ ), the input waveguide is perpendicular to the output waveguides, this bottom substrate contains two sensors. (c) Fabricated sensor with a EURO 10 cent coin, the sensor tested in this work has a radius of  $R = 1.6\text{mm}$  and the length and width of the access waveguides are  $1\text{mm}$  and  $300\ \mu\text{m}$ , respectively. (d) Experimental setup. L: lens MMF: multimode fiber, PD: photodiode, TIA: trans-impedance amplifier.

The experimental setup is shown in Fig. 1(d). A stabilized broadband light source (Thorlabs SLS202) is used for the NDIR sensing experiment. The emitted light is focused by a lens onto multi-mode fiber. The fiber is butt-coupled to the input waveguide of the sensor (fiber to input waveguide distance  $\sim 50\ \mu\text{m}$ ). At the output waveguide

of the sensing arm, light is collimated and re-focused onto a photodiode by two identical lenses ( $f = 1.8\text{mm}$ ), with a band pass filter ( $\lambda_0 = 4.25\mu\text{m}$ , FWHM = 500nm) in between. The lens-filter-lens system is sealed and isolated from the ambient. A customized transimpedance amplifier (TIA) is used to amplify the signal. The reference arm only differs in the optical filter, with pass band centered at  $\lambda_0 = 3.8\mu\text{m}$  (FWHM=500nm), the two arms are otherwise identical. During the measurement, the signal at both arms are simultaneously acquired by two lock-in amplifiers (Standard SR830) with identical settings.

### 3. Experimental results

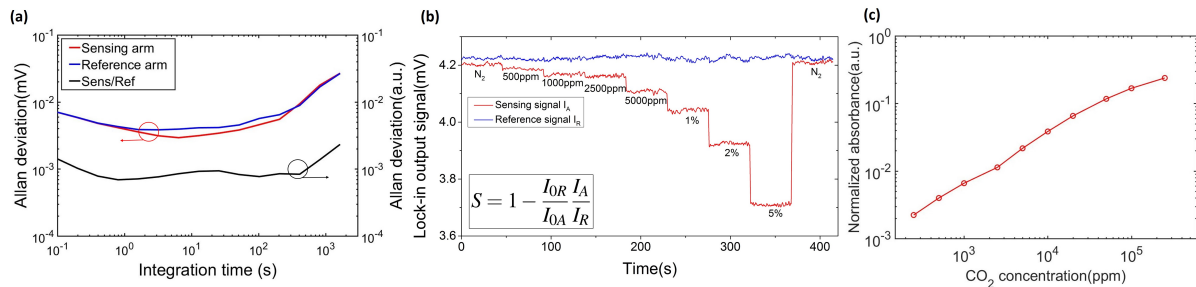


Fig. 2: (a) Allan plot of the sensing and reference arm, as well as the normalized signal (in pure N<sub>2</sub> environment). (b) Step response of the sensor. (c) Normalized absorbance calculated according to the equation in inset of (b).

The experimental results are shown in Fig. 2(a-c). Figure 2(a) shows the Allan deviation plot. One can see that the optimal averaging time (when the Allan deviation of the normalized signal ( $\frac{I_{0A}}{I_{0R}}$ ) is at its minimum, where  $I_{0A}$  and  $I_{0R}$  are the sensing signal and reference signal at zero CO<sub>2</sub>) is approximately 0.7s, and the minimum change in transmission that can be measured is 0.0007 (1  $\sigma$ ). In all following measurements an integration time of 0.3s was used. Figure 2(b) shows the sensor step response when various CO<sub>2</sub> concentrations were applied. It can be seen that the reference signal stays relatively stable while the sensing signal responds to CO<sub>2</sub>. The normalized absorbance was calculated according to the equation in the inset of Fig.2(b) and plotted in Fig.2(c). The limit of detection is approximately 250ppm. The response time of the sensor was measured to be  $\sim 3$ s, by purging with 5% CO<sub>2</sub> and then abruptly shutting the CO<sub>2</sub> flow.

### 4. Conclusion

In summary, a miniaturized integrating-cylinder-based CO<sub>2</sub> sensor is demonstrated in this work. The sensor has a small footprint ( $\sim 5\text{mm} \times 5\text{mm}$ ) and is able to achieve a  $\sim 250\text{ppm}$  CO<sub>2</sub> detection limit, with a response time of only 3 seconds. The use of DRIE based waveguide structures enables mass fabrication, as well as the co-integration of flip-chip integrated midIR LEDs and photodetectors.

The authors acknowledge Melexis and VLAIO for their financial support.

### References

1. S. Neethirajan, D.S. Jayas, and S. Sadistap, "Carbon dioxide (CO<sub>2</sub>) sensors for the agri-food industry-a review" *Food and Bioprocess Technology* **2,2**, 115-121 (2009).
2. A. Wilk, J.C. Carter, M. Chrisp, A.M. Manuel, P. Mirkarimi, J.B. Alameda, and B. Mizaikoff, "Substrate-integrated hollow waveguides: a new level of integration in mid-infrared gas sensing" *Analytical chemistry* **85.23**, 11205-11210 (2013).
3. J. Hodgkinson, R. Smith, W. O. Hah, JR. Saffell, and R.P. Tatam, "Non-dispersive infra-red (NDIR) measurement of carbon dioxide at  $4.2\mu\text{m}$  in a compact and optically efficient sensor" *Sensors and Actuators B: Chemical* **186**, 580-588 (2013).
4. L. Scholz, A. Ortiz Perez, B. Bierer, P. Eaksen, J. Willenstein, and S. Palzer, "Miniature low-cost carbon dioxide sensor for mobile devices" *IEEE Sensors*. **17**, 2889-2895 (2017).
5. S. Moumen, I. I. Raible, A. Krau, and J. Willenstein, "Infrared investigation of CO<sub>2</sub> sorption by amine based materials for the development of a NDIR CO<sub>2</sub> sensor" *Sensors and Actuators B: Chemical* **236**, 1083-1090 (2016).